Dynamics of kink-kink collisions in the double-sine-Gordon system

R. Ravelo, M. El-Batanouny, and C. R. Willis
Department of Physics, Boston University, Boston, Massachusetts 02215

P. Sodano*
Center for Theoretical Physics, Laboratory for Nuclear Science, and Department of Physics, Massachusetts Institute of Technology, Cambridge, Massachusetts 02139
(Received 24 November 1987)

We study the double-sine-Gordon kink-kink collisions in a formalism which employs collective variables to describe the internal oscillations of the kinks and their translational motion in their center-of-mass frame. The equations of motion are solved in the absence of the radiation field and dynamical dressing and the results are compared with numerical molecular-dynamics simulations. We investigate the energy exchange between the translational and internal modes, and a mechanism is proposed to explain the values of the translational velocity at which maximum energy is exchanged between the two modes.

I. INTRODUCTION

The soliton or kink concept has been applied as a paradigm to model nonlinear excitations, localized defects, and particles in many areas of physics: condensed matter,[1,2] quantum optics,[3] plasma physics,[4] particle physics,[5] and even biophysics.[6] However, the nonintegrability of many soliton classes has hampered the explicit treatment of the corresponding multisoliton systems and of the underlying soliton-soliton and soliton-antisoliton interactions. Even in cases of integrable soliton systems, such as the sine-Gordon system, where multisoliton solutions can be readily obtained,[7] it has been rather difficult to extract the relevant details about the nature of the pair interaction process. For example, although the statistical mechanics of the sine-Gordon system has been treated exactly within the transfer-integral method[8] (TIM), and can yield successfully a virial expansion of the free energy in terms of the soliton density, it fails to provide a physical interpretation of the virial coefficients in terms of intersoliton interactions. It has only been recently that direct investigations of these interactions was undertaken. Campbell *et al.*[9,10] have extracted information about kink-antikink interactions from a series of numerical simulations of the ϕ^4 and modified sine-Gordon systems; including the double sine Gordon. Sasaki has investigated the kink-kink collision in the case of the sine-Gordon system[11] in terms of a position shift parameter in an effort to explain the physical significance of the second virial coefficient obtained by TIM.

Thus it is desirable to develop a framework within which it is possible to treat the kink-kink collisions as an interparticle interaction and then investigate the properties of the ensuing interaction potential and its dynamics. It is the purpose of this paper to introduce such a scheme using as example kink-kink collisions in the double-sine-Gordon (DSG) system.[12] The DSG kink has found diverse applications in condensed matter physics: elementary excitations in ^{3}He,[13,14] domain walls in one-dimensional magnetic chains[15] and in ferroelectrics,[16] and very recently as misfit dislocations in the reconstructed (111) surface of gold.[17] It has also been used to model self-induced transparency in nonlinear optics[18] and as an extended object in particle physics.[19] Another interesting aspect of the DSG kink is that it possesses internal dynamical structure[20,21,22] which adds to the richness and complexity of the collision problem and provides a challenging test to the proposed approach.

In the present approach we extend our recently developed Hamiltonian formalism[23] which treats the DSG kink as a particle with one internal degree of freedom to the analysis of the DSG kink-kink (KK) collision. We have used computer simulations as *a posteriori* check on the dynamical details resulting from the formalism. In Sec. II we will present the outline of the DSG collective variable formalism. In Sec. III we derive the Lagrangian and equations of motion and consider the asymptotic motion of the DSG kinks with special consideration to the coupling between the internal and external degrees of freedom. In Sec. IV we present the results of the kink-kink scattering and a comparison with the results obtained from computer simulations. The conclusion is presented in Sec. V and in the Appendix we discuss the importance of using the Lorentz-boosted DSG kink solution in the kink-kink ansatz.

II. COLLECTIVE VARIABLES IN KK SCATTERING

We start with the field Lagrangian

$$L=\int_{-\infty}^{\infty}dx\left[\frac{1}{2}\left[\frac{\partial\Phi}{\partial t}\right]^2-\frac{1}{2}\left[\frac{\partial\Phi}{\partial x}\right]^2-\left[\frac{2\pi}{l_0}\right]^2V(\Phi)\right], \tag{2.1}$$

where

$$V(\Phi)=\frac{4}{1+4|\eta|}\left[\left[1-\cos\frac{\Phi}{2}\right]+\eta(1-\cos\Phi)\right]. \tag{2.2}$$

The potential (2.2) exhibits a variety of structures as the parameter η is varied from $-\infty$ to ∞. Reference 9 gives a detailed analysis of the different regimes and associated solutions as a function of η. $V(\Phi)$ above is normalized such that the bottom of the continuum of small oscillations around the DSG kink solution is always unity. The additional constant terms in the potential are introduced to ensure $V(\Phi)$ vanishes at the absolute minima $\Phi=4n\pi$. In writing (2.2) we have anticipated working in the region $\frac{1}{4}<\eta<\infty$, where there exist only one type of kink which connects two adjacent absolute minima. In this region the potential (2.2) can be rewritten in terms of a new parameter R defined by

$$\eta=\tfrac{1}{4}\sinh^2(R) . \tag{2.3}$$

In terms of this new parameter, the potential (2.2) reads

$$V(\Phi)=\frac{4}{\cosh^2 R}\left[1+\cos\left[\frac{\Phi}{2}\right]\right]+\tanh^2 R(1-\cos\Phi) . \tag{2.4}$$

Figure 1 shows $V(\Phi)$ for $R=1.5$. In this region the static kink solution takes a simple form

$$\sigma_{\mathrm{DSG}}(x-X_0,R)=4\tan^{-1}\left[\frac{\sinh\left[\frac{2\pi}{l_0}(x-X_0)\right]}{\cosh(R)}\right]+4n\pi . \tag{2.5}$$

l_0 above, is the width of the DSG kink and X_0 is the position of its center of mass. Equation (2.5) can be expressed in terms of two sine-Gordon (SG) solitons[23]

$$\sigma_{\mathrm{DSG}}(x-X_0,R)=\sigma_{\mathrm{SG}}\left[\frac{2\pi}{l_0}(x-X_0)+R\right]+\sigma_{\mathrm{SG}}\left[\frac{2\pi}{l_0}(x-X_0)-R\right]+4n\pi , \tag{2.6}$$

where

$$\sigma_{\mathrm{SG}}(x)=4\tan^{-1}(e^x) . \tag{2.7}$$

Equation (2.6) shows that a static DSG kink can be thought of as two bound SG solitons separated by a distance $2R$. The parameter R can then be taken as the separation between the subkinks which make up a DSG soliton.

The moving solution is obtained by Lorentz boosting the static solution (2.5)

$$\sigma_{\mathrm{DSG}}[\gamma(x-X_0-vt),R]=4\tan^{-1}\left[\frac{\sinh\left[\frac{2\pi}{l_0}\gamma(x-X_0-vt)\right]}{\cosh(R)}\right]+4n\pi , \tag{2.8}$$

where $\gamma=(1-v^2)^{-1/2}$. (We work in units where $c=1$. For a detailed discussion of units see Ref. 23.) Equation (2.8) represents a DSG soliton moving with constant velocity v. The separation between the two subkinks of the DSG kink will appear Lorentz contracted to an observer at rest with respect to the moving kink. This is shown explicitly in Fig. 2 which shows the boosted solution (2.8) together with the static solution (2.5). The separation between the subkinks in the moving solution is given by $2R/\gamma$.

In our approach to KK scattering we consider two boosted DSG kinks with centers located at $x=X_1$ and $x=X_2$. Working in the center of mass of the system (c.m.s.) we set $X_1+X_2=0$ and define a relative position coordinate X which is defined as the distance of the kinks centers from the c.m.s. [$x=(x_2-x_1)/2$]. Using a collective variable approach[24] the relative position X and the parameter R in (2.8) are promoted to dynamical variables. In terms of these variables, we write the following ansatz for the DSG kink-kink solution

$$\Phi[\gamma(x-X(t)),R(t),t]=\sigma_{\mathrm{KK}}+\chi(x,t) , \tag{2.9}$$

where

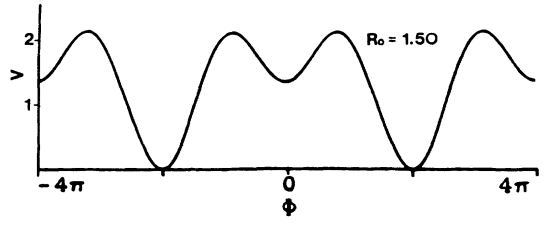

FIG. 1. DSG potential for $R_0=1.50$.

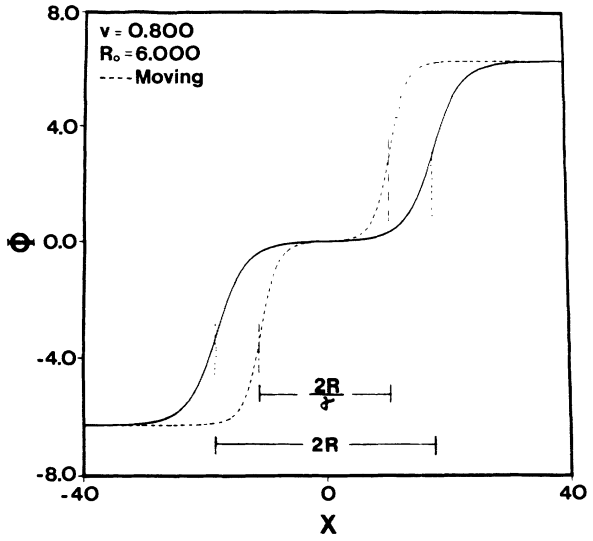

FIG. 2. DSG static solution (2.5) (solid line) and boosted solution (2.8) (broken line) for $R_0=6.0$ and $X_0=0$. The boosted solution appears contracted to an observer at rest with respect to the moving kink.

$$\sigma_{KK}=\sigma_{DSG}[\gamma(x-X(t)),R(t)] +\sigma_{DSG}[\gamma(x+X(t)),R(t)] , \tag{2.10}$$

σ_{DSG} is given by (2.8) with $\gamma=[1-\dot{X}^2(t)]^{-1/2}$.

The basic idea behind this parametrization of the field involves substituting the degrees of freedom of the continuum field Φ by two collective coordinates $X(t)$ and $R(t)$ which describe the translational and internal motion of the kinks, respectively. Equation (2.10) represents two DSG solitons located at $x=X(t)$ and $x=-X(t)$ moving with velocity $\dot{X}(t)$ and $-\dot{X}(t)$ with respect to the c.m.s. The field $\chi(x,t)$ in (2.9) is an independent dynamical variable[23] which includes the dynamical dressing and radiation contribution to the solution. In our treatment of KK scattering it will be set equal to zero. This is done to simplify the analysis of the ensuing equations of motion with the hope that such treatment remains qualitatively correct. As it turns out, the dynamics of KK collisions obtained in the absence of the field χ agree well (within 5% at low velocities) with numerical molecular-dynamics simulations (MDS). The discussion and comparison of the results using this approach will be presented in Sec. IV.

At this point it is important to mention that the boosted solution (2.8) in the ansatz (2.9) is not only the natural choice to use in this type of problem but more importantly, the use of the solution (2.5) with X_0 and R promoted to dynamical variables[23] leads to unphysical results as is shown in the Appendix.

Working in the absence of the field $\chi(x,t)$, (2.9) can be written in a simpler form

$$\Phi(x,X,R,\dot{X})=\sigma_{KK}=4\left[\tan^{-1}\left[\frac{\sinh y}{\cosh A}\right]+\tan^{-1}\left[\frac{\sinh y}{\cosh B}\right]\right]+4n\pi , \tag{2.11}$$

where

$$y=\left[\frac{2\pi}{l_0}\right]\gamma x , \tag{2.12a}$$

$$A=\left[\frac{2\pi}{l_0}\right]\gamma X-R , \tag{2.12b}$$

$$B=\left[\frac{2\pi}{l_0}\right]\gamma X+R , \tag{2.12c}$$

with $\gamma=[1-\dot{X}^2]^{-1/2}$.

Equation (2.11) is used in the field Lagrangian (2.1) to arrive at the equations of motion. This and the approximations involved are described next.

III. THE LAGRANGIAN AND EQUATIONS OF MOTION

The time derivative of (2.11) is explicitly given by

$$\left[\frac{\partial\Phi}{\partial t}\right]=\left[\frac{\partial\sigma_{KK}}{\partial X}\right]\dot{X}+\left[\frac{\partial\sigma_{KK}}{\partial R}\right]\dot{R}+\left[\frac{\partial\sigma_{KK}}{\partial\dot{X}}\right]\ddot{X} . \tag{3.1}$$

In order to simplify the notation the time derivative will be written in terms of a dimensionless variable $Z=(2\pi/l_0)\gamma X$

$$\left[\frac{\partial\Phi}{\partial t}\right]=\left[\frac{\partial\Phi}{\partial Z}\right]\dot{Z}+\left[\frac{\partial\Phi}{\partial R}\right]\dot{R}+\left[\frac{\partial\Phi}{\partial\gamma}\right]\dot{\gamma} . \tag{3.2}$$

Using (3.2), the kinetic term in the field Lagrangian (2.1) reads

$$\tfrac{1}{2}\int_{-\infty}^{\infty}\left[\frac{\partial\Phi}{\partial t}\right]^2dx=\tfrac{1}{2}I_{zz}\dot{Z}^2+\tfrac{1}{2}I_{RR}\dot{R}^2+\tfrac{1}{2}I_{\gamma\gamma}\dot{\gamma}^2 +I_{ZR}\dot{Z}\dot{R}+I_{\gamma R}\dot{\gamma}\dot{R}+I_{\gamma Z}\dot{\gamma}\dot{Z} , \tag{3.3}$$

where

$$I_{ab}=\int_{-\infty}^{\infty}\left[\frac{\partial\Phi}{\partial a}\right]\left[\frac{\partial\Phi}{\partial b}\right]dx . \tag{3.4}$$

The other terms in the Lagrangian are

$$\tfrac{1}{2}\int_{-\infty}^{\infty}\left[\frac{\partial\Phi}{\partial x}\right]^2dx=\left[\frac{2\pi}{l_0}\right]\gamma V_{el} \tag{3.5}$$

and

$$\int_{-\infty}^{\infty}V(\Phi)dx=\left[\frac{l_0}{2\pi}\right]\frac{1}{\gamma}V(Z,R) , \tag{3.6}$$

where

$$V_{el}=8\{2[1+g(R)+g(Z)]+g(Z-R)+g(Z+R)\} \tag{3.7}$$

and

$$V(Z,R)=8\left\{\frac{2}{\cosh^2R_0}\left[\frac{\coth Z}{\tanh R}\right]\left[\frac{R\sinh(2Z)-Z\sinh(2R)}{(\sinh^2Z-\sinh^2R)}\right] +\tanh^2R_0\left[\frac{\coth^2Z}{\tanh^2R}[f(Z+R)+f(Z-R)] +\frac{\coth Z}{\tanh R}(\coth^2Z\coth^2R-1)\left[\frac{Z\sinh(2R)-R\sinh(2Z)}{\sinh^2Z-\sinh^2R}\right]\right]\right\} . \tag{3.8}$$

We have simplified the notation by defining the following functions:

$$g(\xi)=\frac{2\xi}{\sinh(2\xi)}\ , \tag{3.9a}$$

$$f(\xi)=\coth^2(\xi)[1-g(\xi)]\ . \tag{3.9b}$$

The parameter R appearing in the potential (2.4) has been denoted by R_0 in order to distinguish it from the dynamical variable R in (2.8). It is fixed by the physical system and is not allowed to change within a given system.

Due to the dependence of (3.3) on the translational acceleration, the equations of motion generated by such Lagrangian are quite lengthy and of fourth order in the X variable. However, they simplify considerably if one considers collisions at small translational velocities. The simplifying argument behind this approximation goes as follows: since the DSG soliton-soliton interaction is repulsive in nature, the translational velocity of the kinks will be bounded at all times by the initial velocity which we shall denote by v_0. This is, if $\dot{X}(t=-\infty)=v_0$, then $|\dot{X}(t)|\leq|v_0|$ for $-\infty\leq t\leq\infty$. In addition, from energy conservation, the internal motion of each kink will also be bounded by v_0. Furthermore, the duration of the collision is proportional to $\tau\sim l_0/v_0$ (l_0 is the size of each kink) and therefore the accelerations experienced during collision are of the order of v_0^2. If we only keep terms up to order v_0^2, the terms proportional to $\dot{\gamma}$ in the kinetic expression (3.3) can be dropped. The resulting Lagrangian takes the following form:

$$L=\left[\frac{2\pi}{l_0}\right]\left[M_Z\gamma\dot{X}^2+\left[\frac{l_0}{2\pi}\right]^2\frac{1}{\gamma}M_R\dot{R}^2+\left[\frac{l_0}{2\pi}\right]M_{ZR}\dot{X}\dot{R}-V_{\rm el}\gamma-\frac{1}{\gamma}V(Z,R)\right]\ . \tag{3.10}$$

The terms $V_{\rm el}$ and $V(Z,R)$ have been defined in (3.7) and (3.8). The other terms in the Lagrangian are

$$M_Z(Z,R)=\frac{1}{2}\left[\frac{2\pi}{l_0}\right]\gamma\int_{-\infty}^{\infty}\left[\frac{\partial\Phi}{\partial Z}\right]^2dx=8\{2[1-g(Z)+g(R)]-g(Z-R)-g(Z+R)\}\ , \tag{3.11a}$$

$$M_R(Z,R)=\frac{1}{2}\left[\frac{2\pi}{l_0}\right]\gamma\int_{-\infty}^{\infty}\left[\frac{\partial\Phi}{\partial R}\right]^2dx=8\{2[1+g(Z)-g(R)]-g(Z-R)-g(Z+R)\}\ , \tag{3.11b}$$

$$M_{ZR}(Z,R)=\left[\frac{2\pi}{l_0}\right]\gamma\int_{-\infty}^{\infty}\left[\frac{\partial\Phi}{\partial Z}\right]\left[\frac{\partial\Phi}{\partial R}\right]dx=16[g(Z-R)-g(Z+R)]\ , \tag{3.11c}$$

where the function g has been defined in (3.9a). The M_Z term in (3.10) can be combined with the $V_{\rm el}$ term by rewriting $V_{\rm el}$ as follows:

$$V_{\rm el}=M_Z(Z,R)+m(Z,R)\ , \tag{3.12}$$

with

$$m(Z,R)=16[2g(Z)+g(Z-R)+g(Z+R)]\ . \tag{3.13}$$

Employing the same approximation scheme used to drop the $\dot{\gamma}$ terms in (3.3), the dimensionless variable Z can be written as follows:

$$Z=\left[\frac{2\pi}{l_0}\right]\gamma X\ , \tag{3.14a}$$

$$\dot{Z}\simeq\left[\frac{2\pi}{l_0}\right]\gamma\dot{X}\ , \tag{3.14b}$$

$$\ddot{Z}\simeq\left[\frac{2\pi}{l_0}\right]\gamma\ddot{X}\ , \tag{3.14c}$$

where we have neglected all terms of order higher than $\dot{X}^2$. Using (3.12) together with (3.14) in (3.10) we arrive at a *particlelike* Lagrangian in the dimensionless variables Z and R:

$$L=\left[\frac{2\pi}{l_0}\right]\frac{1}{\gamma}\{\alpha^2M_R\dot{R}^2+\alpha^2M_{ZR}\dot{Z}\dot{R}-[M_Z+m\gamma^2+V(Z,R)]\}\ , \tag{3.15}$$

where $\alpha=(l_0/2\pi)$ and from (3.14b) γ is approximately given by

$$\gamma\simeq\sqrt{1+\alpha^2\dot{Z}^2},\quad c=1\ . \tag{3.16}$$

The Lagrangian (3.15) is now a function of Z, $\dot{Z}$, R, and $\dot{R}$. The dependence on X and $\dot{X}$ is only implicit through the definition of Z in (3.14a). The above Lagrangian can be written in a more compact form by defining a velocity-dependent effective potential

$$V_{\rm eff}(Z,\dot{Z},R)=V(Z,R)+M_Z(Z,R)+\gamma^2m(Z,R)\ , \tag{3.17}$$

where the dependence on $\dot{Z}$ is understood to come only from γ.

Figure 3 shows a three-dimensional picture of this effective potential as a function of Z and R for $R_0=2.50$ and $\dot{Z}=0.40$. For large values of Z the potential has its minimum at $R=R_0$. The lateral barriers at both sides of $Z=0$ have their maximum at $Z=R$. This corresponds to a superposition of a SG subkink belonging to one of the DSG kinks with another SG subkink belonging to the other DSG kink. This is more easily seen in Fig. 4, which shows the effective potential as a function of Z for various values of the variable R. The central barrier corresponds to the superposition of all four SG subkinks. The shape of the potential is controlled by the parameter R_0 and the velocity $\dot{Z}$. An increase in translational velocity leads to an increase in the height of the barriers by an amount directly proportional to the increase in γ. On the other hand, an increase in R_0 leads to a decrease in the curvature of the potential along the R axis and vice versa. This can be seen in Fig. 5, which shows a three-

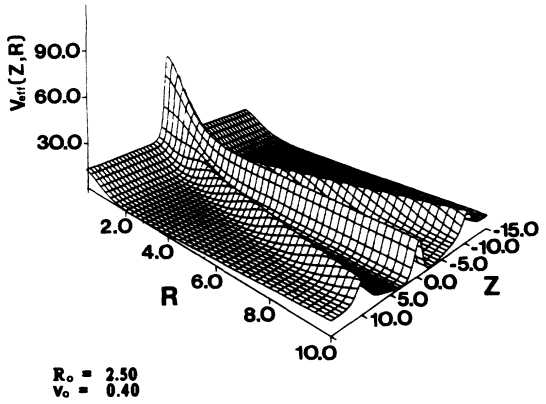

FIG. 3. Perspective plot of the velocity dependent effective potential V_{eff} as a function of the variables $Z=(2\pi/l_0)\gamma X$ and R for $R_0=2.50$ and $\dot{X}=v_0=0.40$.

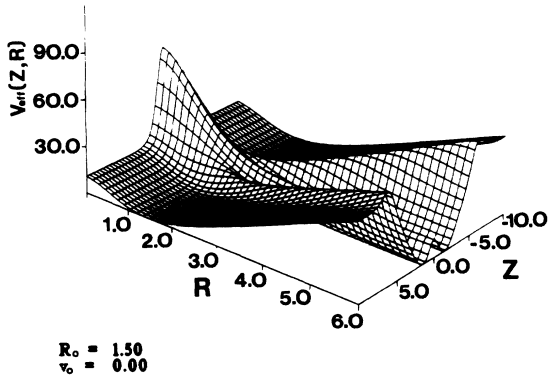

FIG, 5. Perspective plot of the effective intersoliton potential V_{eff} as a function of the variables Z and R for $R_0=1.20$ and $v_0=0.0$ (static case).

dimensional plot of V_{eff} for $R_0=1.50$ and $\dot{Z}=0$ (static case).

It is instructive to look at this effective potential in the limit in which the DSG kinks are very far from each other ($Z\rightarrow\infty$). In this limit, it takes the following very simple functional form:

$$\lim_{Z\rightarrow\infty} V_{\text{eff}}(R=R_0)\equiv\mathcal{V}(R_0)=32\left[1+\frac{2R_0}{\sinh(2R_0)}\right]. \tag{3.18}$$

In the limit in which the kinks are very far away from each other and in the absence of internal oscillations ($R=R_0$), the effective potential reduces to the energy of creation of the two DSG kinks which will be referred to as V_{R_0}. This energy of creation is comprised of the rest masses of four SG subkinks [eight per subkink, in units of $(2\pi/l_0)$] plus the binding energy of the SG subkinks which make up each DSG soliton. This binding energy ($16[2R_0/\sinh(2R_0)]$ per DSG kink) goes to zero as $R_0\rightarrow\infty$. In this limit each DSG soliton disassociates into two free SG solitons.

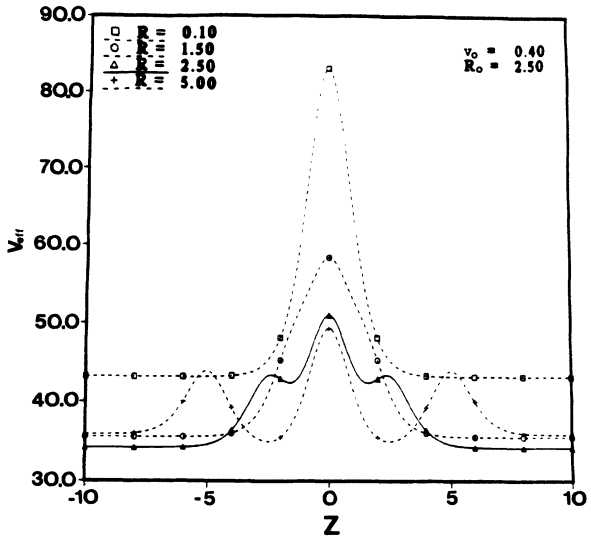

FIG. 4. V_{eff} as a function of the translational variable Z for various values of R for $R_0=2.50$ and $v_0=0.40$.

In terms of this effective potential V_{eff}, the Lagrangian (3.15) takes the following form:

$$L=\left[\frac{2\pi}{l_0}\right]\frac{1}{\gamma}(\alpha^2 M_R\dot{R}^2+\alpha^2 M_{ZR}\dot{Z}\dot{R}-V_{\text{eff}}). \tag{3.19}$$

We obtain the equations of motion for the variables $Z(t)$ and $R(t)$ directly from the Euler-Lagrange equations which follow from (3.19) and by neglecting terms of order higher than v_0^2 [same scheme employed in obtaining Eqs. (3.14b) and (3.14c)]. The distance of the kinks from the c.m.s., $X(t)$ is obtained by inverting Eq. (3.14a). These equations form a pair of second order, coupled differential equations which are solved self-consistently using numerical methods. They are given by

$$\ddot{Z}=\frac{2M_R f_Z-M_{ZR}f_R}{M^2}, \tag{3.20a}$$

$$\ddot{R}=\frac{M_{\text{eff}}f_R-M_{ZR}f_Z}{M^2}, \tag{3.20b}$$

where

$$M_{\text{eff}}=\frac{1}{\gamma^2}V_{\text{eff}}-2m, \tag{3.21a}$$

$$M^2=2M_{\text{eff}}M_R-M_{ZR}^2, \tag{3.21b}$$

and

$$f_Z=[(\partial_Z M_R)-(\partial_R M_{ZR})]\dot{R}^2-\frac{1}{\gamma^2}(\partial_R V_{\text{eff}})\dot{Z}\dot{R}+2(\partial_R m)\dot{Z}\dot{R}-\left[\frac{2\pi}{l_0}\right]^2\left[(\partial_Z V_{\text{eff}})\left[1+\frac{\alpha^2\dot{Z}^2}{\gamma^2}\right]\right]+(\partial_Z m)\frac{\dot{Z}^2}{\gamma^2}, \tag{3.22a}$$

$$f_R = -\left[(\partial_R M_R)\dot{R}^2 + (\partial_Z M_{ZR})\dot{Z}^2 + 2(\partial_Z M_R)\dot{R}\dot{Z} + \left[\frac{2\pi}{l_0}\right]^2 (\partial_R V_{\text{eff}}) \right] . \quad (3.22b)$$

In the limit in which the kinks are far apart, Eqs. (3.20a) and (3.20b) reduce to

$$\mathcal{V}(R)\ddot{Z} = -[\partial_R \mathcal{V}(R)]\dot{Z}\dot{R} , \quad (3.23a)$$

$$2\mathcal{M}_R \ddot{R} = -\partial_R \left[\left[\frac{2\pi}{l_0}\right]^2 \mathcal{V}(R) + \mathcal{M}_R \dot{R}^2 \right] , \quad (3.23b)$$

where

$$\mathcal{V}(R) \equiv \lim_{Z\to\infty} V_{\text{eff}}(Z,R) = 16\left[1+\frac{\tanh^2 R_0}{\tanh^2 R} + \left[1-\frac{\tanh^2 R_0}{\tanh^2 R} + 2\frac{\cosh^2 R}{\cosh^2 R_0}\right]\frac{2R}{\sinh(2R)}\right] , \quad (3.24a)$$

$$\mathcal{M}_R \equiv \lim_{Z\to\infty} M_R(Z,R) = 16\left[1-\frac{2R}{\sinh(2R)}\right] . \quad (3.24b)$$

We can see from Eqs. (3.23a) and (3.23b) that in order to have the kinks move with constant velocity ($\ddot{Z}=0$), internal oscillations must be absent. This leads to the condition $[\partial_R \mathcal{V}(R)]=0$ which has the solution $R=R_0$. R_0 represents the equilibrium separation between the two subkinks of the DSG soliton. Equation (3.23a) gives the asymptotic velocity of the kinks in terms of the effective potential at infinity $\mathcal{V}(R)$ and the initial velocity v_0 [$v_0=\dot{X}(t\to-\infty)$]

$$\dot{X}(t) = v_0 - \left[\frac{\mathcal{V}(R)-\mathcal{V}(R_0)}{\left[\frac{2\pi}{l_0}\right]\gamma\mathcal{V}(R)\mathcal{V}(R_0)}\right] , \quad (3.25)$$

where $\mathcal{V}(R_0)$ above is given by (3.18). The time dependence is implicit in the change of $\mathcal{V}(R)$ with $R(t)$. The term $[\mathcal{V}(R)-\mathcal{V}(R_0)]$ represents the change in the internal energy of the kinks. In the case of small energy transfer, $\mathcal{V}(R)$ can be expanded about R_0 by writing $R(t)=R_0+\rho(t)$ (Ref. 23) with ρ/R_0 small. Carrying out this expansion to order ρ^2 (3.25) reads

$$\dot{X}(t) = v_0 - \left[\frac{\mathcal{M}_R(R_0)\omega_{R_0}^2}{\left[\frac{2\pi}{l_0}\right]^3\gamma\mathcal{V}^2(R_0)}\right]\rho^2(t) . \quad (3.26)$$

In the above expression ω_{R_0} is the frequency of oscillation of the internal mode (assuming harmonic motion) and is given by

$$\omega_{R_0}^2 = \left[\frac{2\pi}{l_0}\right]^2 \frac{[\partial_R^2 \mathcal{V}(R)]}{2\mathcal{M}_R}\bigg|_{R=R_0} . \quad (3.27)$$

IV. KINK-KINK SCATTERING

As it was mentioned in Sec. III, our study of kink-kink interactions is limited to low velocities due to the approximation scheme employed to simplify the equations of motion. The repulsive nature of the intersoliton potential (3.17) does not allow the kinks to go through each other and thus, they simply reflect. In kink-kink collisions we do not find the extremely rich variety of interactions observed by Campbell *et al.*[9] in kink-antikink collisions. However, we do observe energy exchange between the translational and shape modes of the kinks. We will present later in this section a mechanism for explaining maximum energy exchange between these two modes.

Equations (3.20a)–(3.20c) were solved self-consistently using a sixth-order Runge-Kutta-Fehlberg algorithm. The kinks were started far from each other with no internal motion ($\dot{R}=0$) and at various translational velocities. Figure 6 shows a perspective plot of a typical kink-kink collision obtained by solving (3.20) and placing the resulting $X(t)$, $\dot{X}(t)$, and $R(t)$ in the kink-kink ansatz (2.11). In Fig. 7 we show a phase diagram of the internal variable $R(t)$ versus $\dot{R}(t)$ for a collision in which the initial velocity $v_0=0.20$ and the parameter $R_0=2.5$, while in Fig. 8 we show a phase diagram of the separation of the kinks from the c.m.s. $X(t)$ versus $\dot{X}(t)$. We can view the kinks as compressible particles which are deformed during collision, increase their internal energy and reflect with their shape mode undergoing oscillations about R_0 [the minimum of $\mathcal{V}(R)$]. The amplitude of oscillation will depend on the energy transferred to the internal mode. For small energy transfers, the internal motion is harmonic with a frequency given by (3.27). At higher energies, the amplitude increases and higher harmonics of ω_{R_0} will be present. Furthermore, as is shown in Eq. (3.26), these internal oscillations of the kinks, induce oscillatory motion in the translational velocity $\dot{X}$ which oscillates about the average velocity (v_0) with the shape mode frequency. These oscillations are a result of translational momentum conservation.

The numerical simulations method used to check the dynamics of kink-kink collisions involved solving coupled Newtonian equations of motion of particles in a discrete

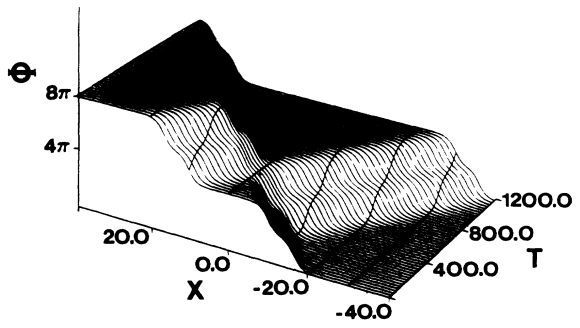

FIG. 6. Perspective plot of kink-kink collision as a function of time. The velocity of approach was set equal to 0.25 and the parameter $R_0=2.50$.

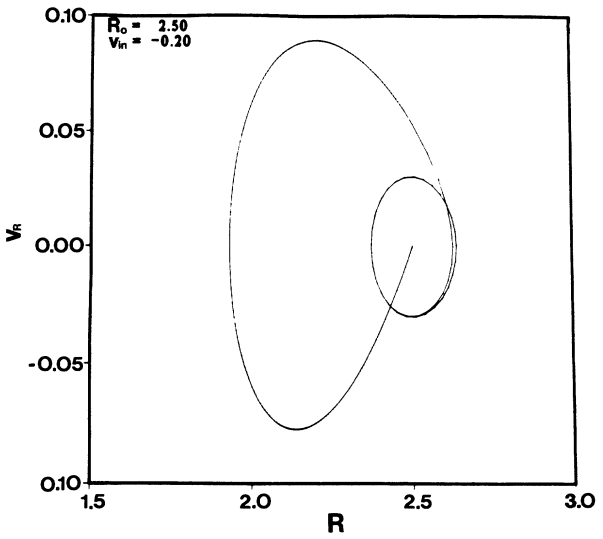

FIG. 7. Phase diagram of the internal mode (R) in DSG kink in kink-kink collision generated by solving Eqs. (3.20a)–(3.20c) with $R_0=2.50$ and $v_0=0.20$.

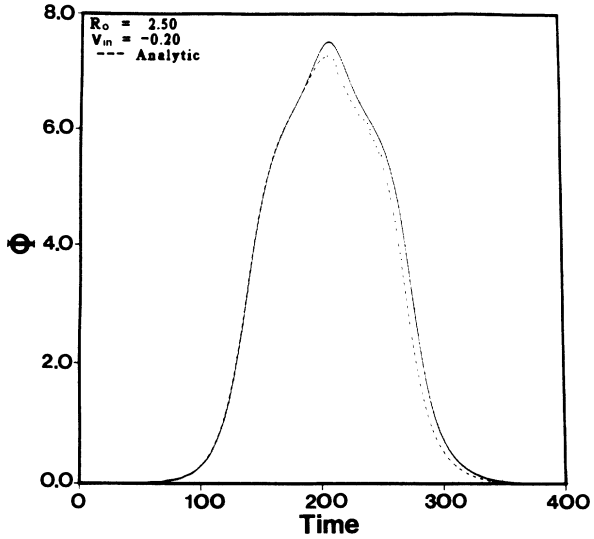

FIG. 9. Plot of the field $\Phi(x=2R_0,t)$ obtained using MDS (solid line) and the ansatz (2.11) with $X(t)$, $\dot{X}(t)$, and $R(t)$ from solving (3.20). $R_0=2.50$ and the initial velocity was set to 0.20 (in units with $c=1$).

chain. The chain was made up of 600 particles and to avoid discreteness effects, the kinks width was made equal to 20 particles. The kinks were started 100 particles apart and the reflection symmetry ($x\rightarrow -x$) of the problem was employed to reduce computational time.

The point $x=2R_0$ of the solution $\Phi(x,t)$, obtained using molecular-dynamics simulations was plotted as a function of time and compared with the ansatz (2.11) evaluated at the same value of x. Figure 9 shows one of such plots. The dotted line represents the analytic result. In all runs generated, the impact parameter (or distance of closest approach between the kinks) in the analytic results was always larger than in the MDS runs. This disagreement lead to an error in the phase shift of the order of 4–8 % for velocities between 0.1 and 0.4. This gives us an estimate of the contribution of the field $\chi(x,t)$ in (2.9) to the overall solution. The MDS show that the radiation is negligible in all cases presented here (small velocities, $R_0=1.5$–4.0). This implies that to lowest order the field $\chi(x,t)$ is a dynamical dressing which takes into account the overlap of the two DSG kinks. In order to further investigate the role of $\chi(x,t)$, the shape mode parameter $R(t)$ and the separation between the kinks $X(t)$, were computed from MDS data and compared with the solution of Eqs. (3.20a) and (3.20b). Figures 10 and 11 show one of such comparisons. The dotted line again represents the analytic result. The very good agreement demonstrates that the collective variables Eqs. (3.20a) and (3.20b) which were obtained in the absence of the field $\chi(x,t)$ are a very accurate representation of the exact MDS results. In Fig. 10, the analytic curve is shifted relative to the MDS curve by an amount equal to the phase-shift error caused by neglecting χ. The omission of the dynamical dressing to lowest order is mostly responsible for the difference in the impact parameter observed in Fig. 9. In order to remove the disagreement in the impact parameter and the phase shift one needs to include the χ contribution to the solution (2.9) to the same order as Eqs. (3.20a) and (3.20b). Doing this, however, will not change $R(t)$ and $X(t)$ and therefore will have no effect on the energy transfer.

Let us now turn to the energy-transfer mechanism. The energy transfer between the translational and internal modes was computed from the asymptotic internal motion of the kinks and compared with the initial translational energy. This was done for several values of the parameter R_0 and initial translational velocities v_0.

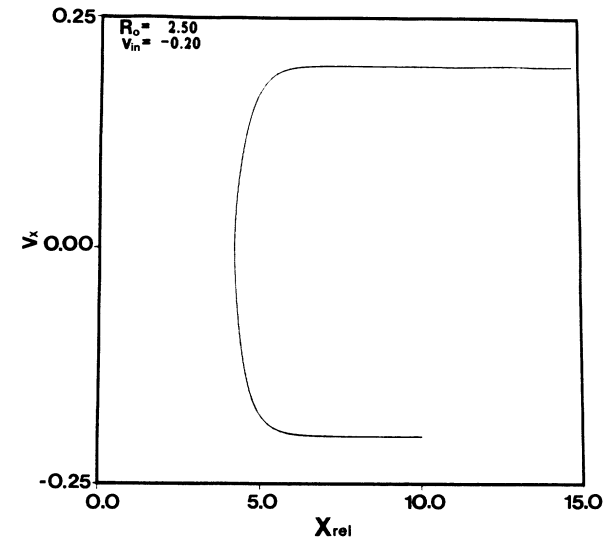

FIG. 8. Phase diagram of the translational mode (X) in kink-kink collision generated from (3.20) with $R_0=2.50$ and $v_0=0.20$.

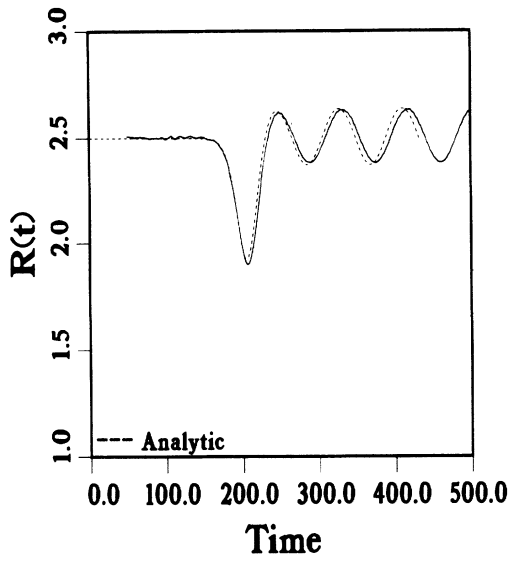

FIG. 10. Plot of the internal mode $R(t)$ obtained using MDS (solid line) and the analytic solution from Eq. (3.20b) (dotted line). $R_0=2.50$ and $v_0=0.20$.

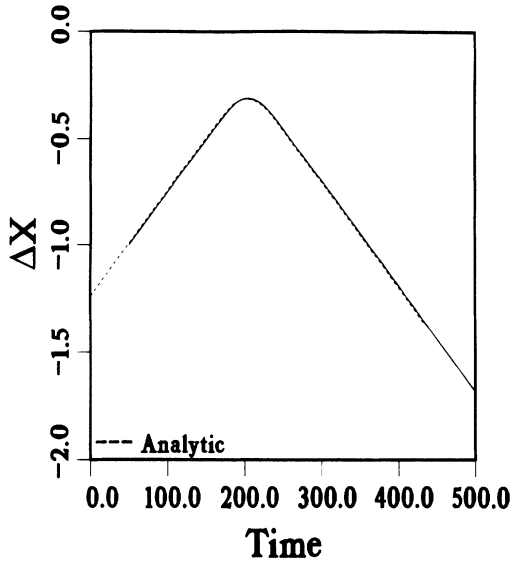

FIG. 11. Plot of the distance between the kinks $X(t)$ obtained using MDS (solid line) and the analytic solution from Eq. (3.20a) (dotted line). $R_0=2.50$ and $v_0=0.20$. ΔX is the separation between the kinks normalized to the initial separation.

The results are presented in Fig. 12, which shows the ratio of the internal energy (E_r) to initial translational energy (E_t) as a function of initial translational velocity. We observe that the energy transfer between the translational and shape modes is small, of the order of 2–4 % of the initial translational energy of the kinks. The mechanism that leads to maximum energy transfer can be explained by assuming the interaction between the kinks takes place in a time which is close or equal to the period of oscillation of the shape mode of the kinks. The translational motion and the internal motion would then be *in-phase*. In order to find an approximate expression for the time during which the kinks interact, we define a *region of interaction* in which the kinks *feel* each other strongly. In this region the kinks will be compressed and the translational velocity will change rapidly. The length of this region will depend on the size of the kinks and we will approximate it by $\alpha l_0+\beta R_0$ (R_0 is measured in units of $l_0/2\pi$), where α and β are parameters to be determined empirically from the data. The time T which the kinks spent in this region will approximately be given by

$$T=\frac{\alpha l_0+\beta R_0}{v_0} . \tag{4.1}$$

The condition which leads to maximum energy transfer relates this time T with the frequency of oscillation of the shape mode of the DSG kinks [ω_{R_0} in Eq. (3.27)]. Therefore, maximum energy transfer will take place when

$$T\simeq\frac{2\pi}{\omega_{R_0}} . \tag{4.2}$$

Combining (4.1) with (4.2) leads to an equation for the initial velocity at which there is maximum energy transfer

$$v_0=(\alpha l_0+\beta R_0)\left[\frac{\omega_{R_0}}{2\pi}\right] . \tag{4.3}$$

The parameters α and β which best fit the data are found to be equal to $\alpha/2\pi=0.212$, $\beta/2\pi=0.294$.

Figure 13 shows a plot of the values of the velocity at which one finds maximum energy transfer using the present formalism as a function of the parameter R_0. In the same plot, we have included a curve generated using Eq. (4.3) above. The agreement is quite good for values of $R_0\leq 4.0$.

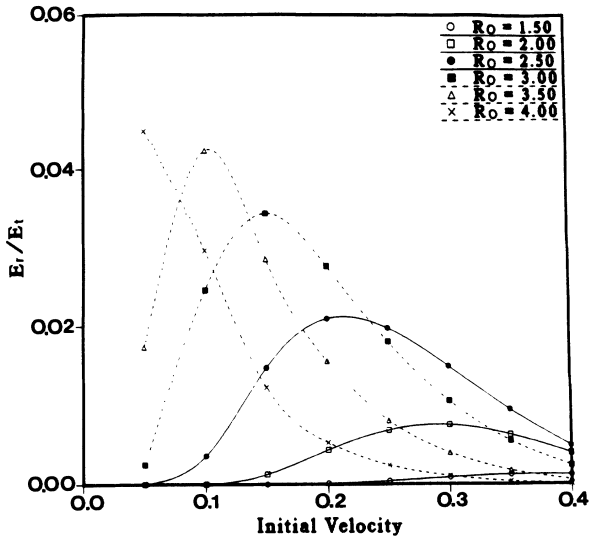

FIG. 12. Ratio of internal energy to initial translational energy as a function of initial kink velocity for various values of R_0.

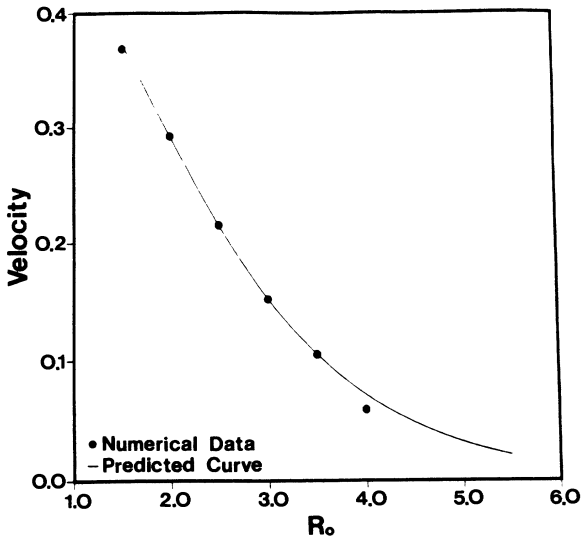

FIG. 13. Plot of velocity of approach at which there is maximum energy exchanged as a function of the parameter R_0. The solid line is generated by using Eq. (4.4) with $\alpha/2\pi=0.212$ and $\beta/(2\pi)=0.294$.

V. SUMMARY AND CONCLUSIONS

In this paper we have developed a theoretical formalism for describing DSG kink-kink interactions. We introduced two collective coordinates, $X(t)$ and $R(t)$ which describe the translational and internal motion of the kinks, respectively. We introduced an ansatz for the DSG kink-kink solution which employs two DSG boosted solutions and a radiation field $\chi(x,t)$. The relativistic Lagrangian obtained in the absence of the field χ was simplified by working at small velocities and defining a new variable $Z=(2\pi/l_0)\gamma X(t)$. The coupled equations of motion for the variables $Z(t)$ and $R(t)$ were solved for various initial conditions and the energy in the internal and translational mode was computed in the asymptotic limit in which the kinks are very far apart. Even though we neglect the radiation and dynamical dressing contributions, these equations provide us with a powerful tool to investigate the dynamics and energy exchange mechanism in kink-kink collisions. The results obtained using this formalism were compared to MDS and good agreement was observed in all cases studied. The radiation was negligible and to lowest order the field χ is the dynamical dressing which takes into account the overlap between the DSG kinks. The omission of the dynamical dressing leads to an error of 4–8 % in the phase shift.

The energy exchange between translational and internal modes was observed to be small for all values of R_0 (2–4 % of the initial translational energy). A condition was found which predicts the velocity at which energy transfer is a maximum. This condition defines a region of interaction whose length can be approximated by $(\alpha l_0+\beta R_0)$ with $\alpha/2\pi=0.212$ and $\beta/(2\pi)=0.294$.

ACKNOWLEDGMENTS

This work is supported by the U.S. Department of Energy under Contract No. DE-FG02-85ER45222. One of the authors P.S. would like to thank North Atlantic Treaty Organization (NATO) for financial support.

APPENDIX

The purpose of this appendix is to show that to get the equation of motion for the collective variable X correct to order $\dot{X}^2$ in any kink problem where the original nonlinear field equation is Lorentz invariant, it is necessary to assume the Lorentz boosted solution and not the static solution for σ. We consider the simplest case of a single DSG kink moving with uniform center of mass velocity $\dot{X}=v_0$. If we assume the static solution

$$\sigma_{\rm DSG}=\sigma_{\rm SG}\left[\frac{2\pi}{l_0}(x-X)+R\right]+\sigma_{\rm SG}\left[\frac{2\pi}{l_0}(x-X)R\right]+4n\pi\ ,$$

and substitute in Eq. (2.1) for L and integrate, we obtain the following Lagrangian:

$$L=\tfrac{1}{2}M_X(R)\dot{X}^2+\tfrac{1}{2}M_R(R)\dot{R}^2-V_R(R)\ , \tag{A1}$$

where

$$V_R(R)\equiv\int\left[\left[\frac{2\pi}{l_0}\right]^2V(\sigma)+\left[\frac{\partial\sigma}{\partial X}\right]^2\right]dx\ .$$

However, if we substitute instead the Lorentz-boosted ansatz

$$\sigma_{\rm DSG}\left[\frac{2\pi}{l_0}\gamma(x-X),R\right]=\sigma_{\rm SG}\left[\frac{2\pi}{l_0}\gamma(x-X)+R\right]+\sigma_{\rm SG}\left[\frac{2\pi}{l_0}\gamma(x-X)-R\right]$$

into Eq. (2.1) for L we obtain

$$L=\gamma^{-1}[M_R(R)\dot{R}^2-V_{\rm eff}(R)]=\gamma^{-1}\left[M_R(R)\dot{R}^2-M_X(R)-\left[\frac{2\pi}{l_0}\right]^2V(\sigma)\right]\ , \tag{A2}$$

where the second equality follows from the definition

$$V_{\rm eff}\equiv M_X(R)+\left[\frac{2\pi}{l_0}\right]^2V(R)\ . \tag{A3}$$

The Lagrangian of Eq. (A2) is Lorentz invariant in the center-of-mass variable X and the internal variable R, is treated nonrelativistically. The most important consequence of the difference between the correct Eq. (A2) and the incorrect Eq. (A1) is the value of the separation R between the two subkinks as predicted by the two equations. If we consider the case $\dot{R}=0$ so that we have a uniformly translating kink, then the value of R is obtained from the equation of motion $\partial L/\partial R=0$. For Eq. (A1) we obtain

$$\frac{\partial}{\partial R}[\tfrac{1}{2}M_X(R)v_0^2 - V_R(R)] = 0 \ , \tag{A4}$$

while for Eq. (A2) we obtain

$$\frac{\partial}{\partial R} V_{\text{eff}}(R) = 0 \ ,$$

which gives

$$R_{\min} = R_0 \ . \tag{A5}$$

We see Eq. (A4) gives the incorrect result that $R_{\min}$ depends on v_0, i.e., the value of the separation of the kinks for a uniformly moving DSG is different for different inertial frames which cannot be. On the other hand, Eq. (A5) gives the correct result that a uniformly moving kink has the correct minimum value of R, namely R_0, independent of the velocity of the kink. In conclusion we observe that the case of the static kink solution instead of the boosted kink solution is seriously in error already at terms of order $\dot{X}^2$.

*Permanent address: Dipartimento di Fisica, Università degli Studi di Perugia, via Elce di Sotto 10, I-06100, Perugia, Italy.

[1] *Nonlinearity in Condensed Matter Physics,* edited by A. R. Bishop, D. A. Campbell, P. Kumar, and S. Trullinger (Springer, New York, 1987).

[2] *Solitons in Condensed Matter Physics,* edited by A. R. Bishop and Schneider (Springer, New York, 1978).

[3] R. K. Bullough, P. J. Caudrey, and H. M. Gibbs, in *Solitons,* edited by R. K. Bullough and P. J. Caudrey (Springer, New York, 1980); R. K. Bullough and P. J. Caudrey, in *Nonlinear Evaluation Equations Solvable by the Spectral Transform,* edited by F. Calogero (Pitman, London, 1978).

[4] R. K. Dodd, J. C. Eilenbeck, J. D. Gibbon, and H. C. Morris, *Solitons and Nonlinear Wave Equations* (Academic, New York, 1982).

[5] R. Rajaraman, *Solitons and Instantons* (North-Holland, New York, 1982).

[6] A. C. Scott, Phys. Rev. A **26**, 578 (1982).

[7] G. Eilenberger, *Solitons* (Springer-Verlag, New York, 1983).

[8] N. Gupta and B. Sutherland, Phys. Rev. A **14**, 1790 (1976).

[9] D. K. Campbell, M. Peyrard, and P. Sodano, Physica **19D**, 165 (1986).

[10] D. K. Campbell, J. F. Schonfeld, and C. A. Wingate, Physica **9D**, 1 (1983).

[11] K. Sasaki, Phys. Rev. B **33**, 7743 (1986).

[12] P. Sodano, *Proceedings of the Conference on Quantum Field Theory: Past, Present and Future, 1985* (North-Holland, Amsterdam, 1986).

[13] K. Maki and P. Kumar, Phys. Rev. B **14**, 118 (1976); **14**, 3290 (1976).

[14] Y. Shiefman and P. Kumar, Phys. Scr. **20**, 435 (1979).

[15] K. M. Leung, Phys. Rev. B **27**, 2877 (1983); J. A. Holyst and A. Sukiennicki, *ibid.* **28**, 4062 (1983).

[16] O. Hudak, J. Phys. C **16**, 2641 (1983); **16**, 2659 (1983).

[17] M. El-Batanouny, S. Burdick, K. M. Martini, and P. Stancioff, Phys. Rev. Lett. **58**, 2762 (1987).

[18] S. Duckworth, R. K. Bullough, P. J. Caudrey, and J. D. Gibbon, Phys. Lett. **57A**, 19 (1976).

[19] T. Uchiyama, Phys. Rev. D **14**, 3520 (1976).

[20] S. de Lillo and P. Sodano, Lett. Nuovo Cimento **37**, 380 (1983).

[21] P. Sodano, M. El-Batanouny, and C. Willis, Phys. Rev. B **34**, 4936 (1986).

[22] S. Burdick, M. El-Batanouny, and C. R. Willis, Phys. Rev. B **34**, 6575 (1986); *ibid*; **36**, (1987).

[23] C. Willis, M. El-Batanouny, S. Burdick, R. Boesch, and P. Sodano, Phys. Rev. B **35**, 3496 (1987).

[24] E. Tomboulis, Phys. Rev. D **12**, 1678 (1975).

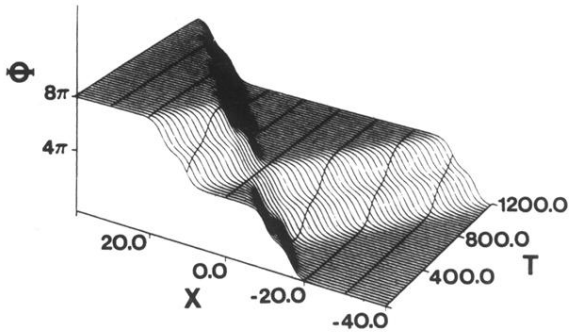

FIG. 6. Perspective plot of kink-kink collision as a function of time. The velocity of approach was set equal to 0.25 and the parameter $R_0 = 2.50$.